

Instability in the dense supernova neutrino gas with flavor-dependent angular distributions

Alessandro Mirizzi¹ and Pasquale Dario Serpico²

¹*II Institut für Theoretische Physik, Universität Hamburg,
Luruper Chaussee 149, 22761 Hamburg, Germany*

²*LAPTh, Univ. de Savoie, CNRS, B.P.110, Annecy-le-Vieux F-74941, France*

The usual description of self-induced flavor conversions for neutrinos (ν 's) in supernovae is based on the simplified assumption that all the ν 's of the different species are emitted “half-isotropically” by a common neutrinosphere, in analogy to a blackbody emission. However, realistic supernova simulations show that ν angular distributions at decoupling are far from being half-isotropic and, above all, are flavor-dependent. We show that flavor-dependent angular distributions may lead to crossing points in the angular spectra of different ν species (where $F_{\nu_e} = F_{\nu_x}$ and $F_{\bar{\nu}_e} = F_{\bar{\nu}_x}$) around which a new multi-angle instability can develop. To characterize this effect, we carry out a linearized flavor stability analysis for different SN neutrino angular distributions. We find that this instability can shift the onset of the flavor conversions toward low-radii and produce a smearing of the splitting features found with trivial ν emission models. As a result the spectral differences among ν 's of different flavors could be strongly reduced.

PACS numbers: 14.60.Pq, 97.60.Bw

Introduction.— The neutrino flux emitted from a core-collapse supernova (SN) represents a powerful tool to get valuable information about the mixing parameters and the dynamics of the exploding stellar core. In this context, renewed attention is being paid to collective features of flavor transformations [1, 2] induced by ν - ν self-interactions [3, 4] in the deepest SN regions, near the neutrino-sphere (see [5] for a recent review). In particular, it has been claimed that the self-induced “spectral splits” would be observable in the ν burst from the next galactic SN, allowing to get crucial information about the unknown ν mass ordering (see, e.g., [6]).

The development of these self-induced effects crucially depends on the inner boundary conditions fixed for the flavor evolution, e.g. on the ν initial energy and angular distributions. In this context, all the recent numerical simulations have been based on the so-called “bulb model” (see, e.g. [1, 7]). Assuming that the ν trapping region at high matter density can be decoupled from the region at lower density where flavor conversions would start, ν 's of different species are considered as emitted “half-isotropically” (i.e. with all outward-moving angular modes equally occupied and all the backward-moving modes empty) by a common spherical “neutrinosphere,” in analogy with a blackbody emission. However, this simplified toy-model may not capture important features of the SN ν emission. In particular, the transition between the isotropic ν emission in trapping regime (at a higher matter density) to the forward-peaked free streaming (at a lower matter density) does not necessarily imply a radius where the ν angular distributions are half-isotropic (see, e.g., [8, 9]). Moreover, the different ν species decouple at different radii. Therefore, the physical last-scattering neutrinospheres for the different species would not coincide. Then, fixing a common neutrinosphere as inner boundary for the flavor evolution, one would realistically find there different angular distributions for the

different ν species. In particular, since the $\bar{\nu}_e$'s and ν_x 's decouple at smaller radii with respect to ν_e 's their distributions are more forward-peaked.

The presence of non-trivial angular distributions was claimed in [10] to produce a multi-angle instability in the self-induced flavor evolution of a toy model of ν gas. However, in that seminal paper the author warned readers not to draw firm conclusions for the realistic SN ν case from his analysis performed with a small number of angular modes, before having explored this case with large-scale numerical simulations. Stimulated also by his intriguing hint, we decided to begin a systematic study of this issue. We find that as long as flavor universality is not broken in the ν angular distributions, only minor quantitative effects appear in the evolution with respect to the half-isotropic case. Conversely, flavor-dependent angular distributions can dramatically affect the conversions of the dense SN ν gas. We relate this behavior to the presence of crossing points in the angular spectra of different ν species (i.e., at emission angles for which $F_{\nu_e} = F_{\nu_x}$ and $F_{\bar{\nu}_e} = F_{\bar{\nu}_x}$). It is known that ν energy spectra presenting crossing points in the energy variable can develop instabilities around them [11]. This effect has been analytically understood performing a linearized stability analysis of the ν equations of motion [12]. Here, applying the same analysis, we find that an analogous effect occurs when the angular spectra of different flavors present crossing points. As a consequence, this multi-angle instability can lead to a wash-out of the splitting features found assuming a half-isotropic ν emission.

Energy and angular distributions.— In order to perform our study of the multi-angle instability we have to fix our ν emission models. Our main goal would be to remove the bulb-model approximation of a half-isotropic neutrino angular distribution at the neutrinosphere, equal for all the species. In order to introduce ν angular distributions, it is convenient to parameterize

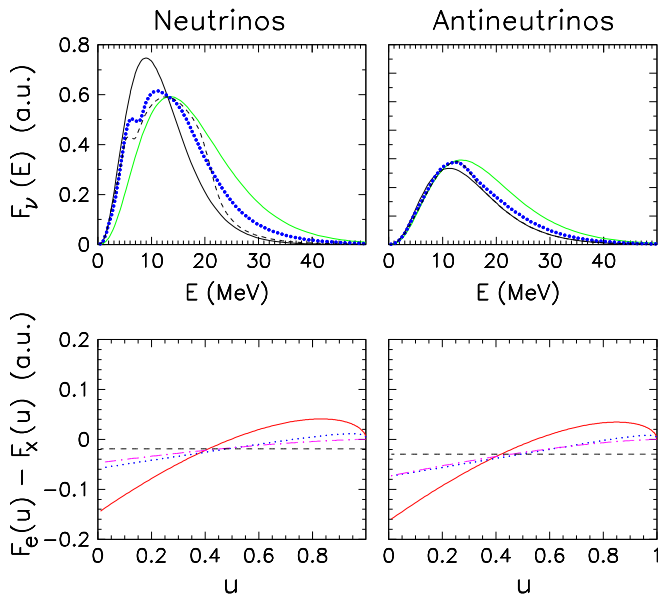


FIG. 1: Upper panels: Multi-angle flavor evolution for ν 's (left panel) and $\bar{\nu}$'s (right panel). Energy spectra initially for ν_e (black continuous curves) and ν_x (light continuous curves) and after collective oscillations for ν_e with half-isotropic angular distribution (dashed curves) and for an angular distribution with $\beta_e = 1.0$, $\beta_x = 1.5$ (thick dotted curves). Lower panels: Difference of the energy-integrated angular spectra $F_{\nu_e}(u) - F_{\nu_x}(u)$ for ν 's (left panel) and $\bar{\nu}$'s (right panel) at the neutrinosphere for the half-isotropic case $\beta_e = \beta_x = 0.0$ (dashed curves) and for the cases with $\beta_e = 1.0$, $\beta_x = 1.5$ (dotted curves), $\beta_e = 1.0$, $\beta_x = 3.0$ (continuous curves) and $\beta_e = \beta_x = 3.0$ (dash-dotted curves).

every angular mode in terms of its emission angle ϑ_R relative to the radial direction of the neutrinosphere, that here we schematically fix at $R = 10$ km. A further simplification is obtained if one labels the different angular modes in terms of the variable $u = \sin^2 \vartheta_R$, as in [12, 13]. Note that for an half-isotropic emission at the neutrinosphere the ν angular distribution of the radial fluxes is a box spectrum in $0 \leq u \leq 1$ [13].

We remark that energy and angular distributions of SN ν 's entering the ν number fluxes $F_{\nu_\alpha}(E, u)$, integrated over a sphere of radius r , are not independent of each other. However, here we schematically assume that the angular distributions are energy independent. Then, we can factorize the ν flux of each flavor as $F_{\nu_\alpha}(E, u) = N_{\nu_\alpha} \times \varphi_{\nu_\alpha}(E) \times U_{\nu_\alpha}(u)$. The function $\varphi_{\nu_\alpha}(E)$ is the normalized ν energy spectrum ($\int dE \varphi_{\nu_\alpha}(E) = 1$), which we will parametrize for the different flavors with deformed Maxwell-Boltzmann distributions, as suggested by SN simulations [14]. The function $U_{\nu_\alpha}(u)$ is the normalized angular distribution ($\int du U_{\nu_\alpha}(u) = 1$). We fix the neutrino average energies at $(\langle E_{\nu_e} \rangle, \langle E_{\bar{\nu}_e} \rangle, \langle E_{\nu_x} \rangle) = (12, 15, 18)$ MeV. Concerning the possible ν flux ordering we consider a case representative of the cooling phase [16], i.e. $N_{\nu_e} : N_{\bar{\nu}_e} : N_{\nu_x} = 1.13 : 1.00 : 1.33$. According to this choice, in the upper panels of Figure 1

are represented the initial fluxes for ν_e (continuous black curves) and ν_x (continuous light curves) for ν 's (left panels) and $\bar{\nu}$'s (right panels) respectively.

A systematic characterization of the ν angular distributions at different radii in SNe is lacking in literature. Therefore, inspired by an inspection of some real angular distributions [15], we use a simple toy model to capture the main deviations with respect to the half-isotropic bulb model, where $U_{\nu_\alpha} = 1$ for all the ν species. In particular, we choose forward-peaked distributions $U_{\nu_\alpha}(u) \propto (1 - u)^{\beta_\alpha/2}$. For simplicity in the following we assume $U_{\nu_e} = U_{\bar{\nu}_e}$. In the lower panels of Figure 1 we plot the energy-integrated spectral difference $F_{\nu_e}(u) - F_{\nu_x}(u)$ for ν 's (left panels) and the analogous one for $\bar{\nu}$'s (right panels) for four representative (β_e, β_x) cases. Namely we compare the half-isotropic case ($\beta_e = \beta_x = 0$, dashed curves) with three non-trivial angular distributions: $\beta_e = 1.0$, $\beta_x = 1.5$ (dotted curves), $\beta_e = 1.0$, $\beta_x = 3.0$ (continuous curves), and $\beta_e = \beta_x = 3.0$ (dash-dotted curves). One realizes that in the half-isotropic case $\beta_e = \beta_x = 0.0$ and in the flavor universal case $\beta_e = \beta_x = 3.0$, the differences of angular spectra do not present any crossing point in the angular variable, while in the other two cases, the spectra present a crossing point at finite $0 < u < 1$, where $F_{\nu_e}(u) = F_{\nu_x}(u)$. We will show that crossing points in the energy-integrated angular spectra will produce a significant speed-up of the multi-angle instability in the ν flavor conversions.

Setup of the flavor evolution.— Our description of the non-linear ν flavor conversions is based on a two-flavor oscillation scenario. For simplicity, we refer to the cases studied in [16] in which three-flavor effects associated with the solar sector are sub-leading. In this situation, self-induced oscillations are driven by the atmospheric mass-square difference $\Delta m_{\text{atm}}^2 = m_3^2 - m_{1,2}^2 \simeq 2.0 \times 10^{-3} \text{ eV}^2$ and by a small (matter suppressed) in-medium mixing $\Theta_m = 10^{-3}$ [17]. We refer to late-time cooling phase ($t \gtrsim 1$ s) where the electron density n_e is smaller than the ν one n_ν and then has a subleading role on the development of the collective oscillations [18]. Apart from the mixing suppression, we neglect the sub-leading matter effects in the flavor evolution. We will refer to the inverted mass hierarchy ($\Delta m_{\text{atm}}^2 < 0$).

Following [12], we write the equations of motion for the flux matrices $\Phi_{E,u}$ as function of the radial coordinate. The diagonal $\Phi_{E,u}$ elements are the ordinary number fluxes $F_{\nu_\alpha}(E, u)$. We normalize the flux matrices to the total $\bar{\nu}_e$ number flux $N_{\bar{\nu}_e}$ at the neutrinosphere. Conventionally, we use negative E and negative number fluxes for $\bar{\nu}$'s. The off-diagonal elements, which are initially zero, carry a phase information due to flavor mixing. Then, the equations of motion read $i\partial_r \Phi_{E,u} = [H_{E,u}, \Phi_{E,u}]$ with the ν - ν Hamiltonian [3, 4, 12]

$$H_{\nu\nu} = \frac{\sqrt{2}G_F}{4\pi r^2} \int_{-\infty}^{+\infty} dE' \int_0^1 du' \left(\frac{1 - v_u v_{u'}}{v_u v_{u'}} \right) \Phi_{E',u'} . \quad (1)$$

The factor proportional to the neutrino velocity $v_{u,r} =$

$(1 - uR^2/r^2)^{1/2}$ [13] implies “multi-angle” effects for neutrinos moving on different trajectories [1, 3, 4]. In order to properly simulate numerically this effect one needs to follow a large number [$\mathcal{O}(10^3)$] of interacting ν modes.

Stability condition.— In order to achieve a deeper understanding of the multi-angle instability, triggered by non-trivial angular distributions, we find particularly useful to apply to our problem the linearized stability analysis recently worked out in [12]. This method allows us to determine the onset of the flavor conversions, seeking an exponentially growing solution in the eigenvalue equations, associated with the linearized equations of motion for the ν ensemble.

In order to perform the stability analysis we closely follow the prescriptions presented in [12] and summarized in the following. At first we switch to the frequency variable $\omega = \Delta m_{\text{atm}}^2/2E$ and we introduce the neutrino flux difference distributions $g_{\omega,u} \equiv g(\omega,u) = |d\omega/dE|[F_{\nu_e}(E(\omega),u) - F_{\nu_x}(E(\omega),u)]$, normalized to the total $\bar{\nu}_e$ flux at the neutrinosphere. Note that $g_{\omega,u}$ is defined also for negative ω , where it represents the difference of fluxes in the antineutrino sector in the opposite ordering. Then, we write the flux matrices as [12]

$$\Phi_{\omega,u} = \frac{\text{Tr}\Phi_{\omega,u}}{2} + \frac{g_{\omega,u}}{2} \begin{pmatrix} s_{\omega,u} & S_{\omega,u} \\ S_{\omega,u}^* & -s_{\omega,u} \end{pmatrix}, \quad (2)$$

where $\text{Tr}\Phi_{\omega,u}$ is conserved and then irrelevant for the flavor conversions, and the initial conditions for the “swapping matrix” in the second term on the right-hand side are $s_{\omega,u} = 1$ and $S_{\omega,u} = 0$. Self-induced flavor transitions start when the off-diagonal term $S_{\omega,u}$ exponentially grows. In the small-amplitude limit $|S_{\omega,u}| \ll 1$, and at far distances from the neutrinosphere $r \gg R$, the linearized evolution equations for $S_{\omega,u}$ lead to an eigenvalue equation [12]

$$(\omega + u\epsilon\mu - \Omega)Q_{\omega,u} = \mu \int du' d\omega' (u+u')g_{\omega',u'}Q_{\omega',u'}, \quad (3)$$

for the eigenvector $Q_{\omega,u}$, obtained writing the solution of the linearized equation $S_{\omega,u} = Q_{\omega,u}e^{-i\Omega r}$. Here we introduced the complex frequency $\Omega = \gamma + i\kappa$ and the parameter $\epsilon = \int du d\omega g_{\omega,u}$ quantifying the “asymmetry” of the neutrino spectrum, normalized to the total $\bar{\nu}_e$ number flux. For our specific choice of ν spectra, it results $\epsilon = 0.13$. The ν - ν interaction strength is given by

$$\mu = \frac{\sqrt{2}G_F N_{\bar{\nu}_e} R^2}{4\pi r^2}. \quad (4)$$

For our SN model, it results $\mu(R) = 4.7 \times 10^{-4} \text{ km}^{-1}$. A solution of Eq. (3) with $\kappa > 0$ would indicate an exponential increasing $Q_{\omega,u}$, i.e. an instability. When an instability occurs, for a given angular mode u_0 the function $|Q_{\omega,u_0}|$ is a Lorentzian [11], centered around a *resonance frequency* $\omega = \gamma - u\epsilon\mu$, and with a width κ .

Flavor conversions— In order to illustrate the effect of the angular distributions, in Fig. 1 (upper panels) we

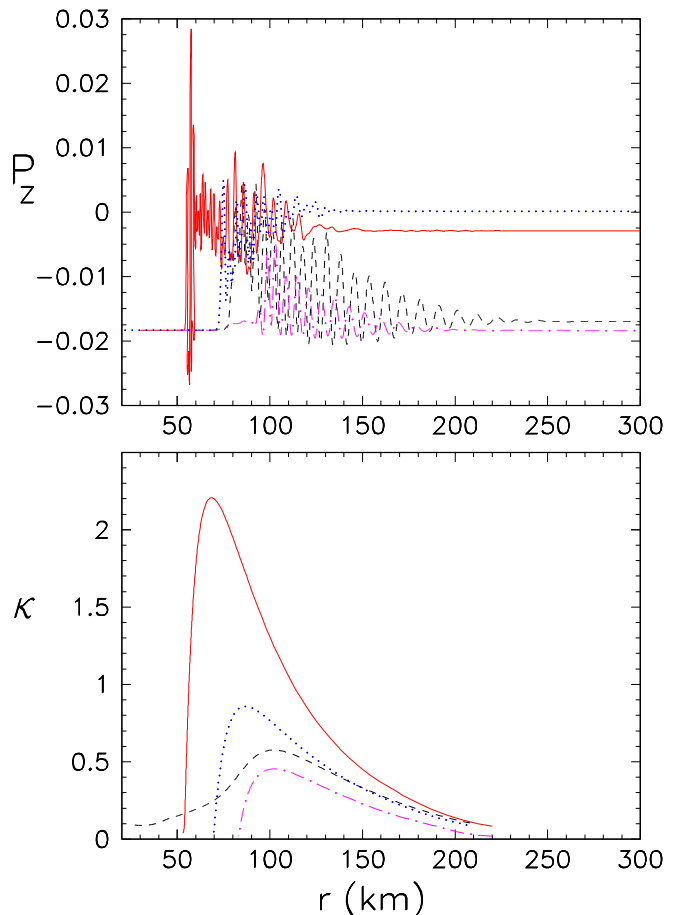


FIG. 2: Upper panel: Radial evolution of the integrated z -component of the polarization vector P_z for ν 's for the half-isotropic case (dashed curve) and for angular distributions with $\beta_e = 1.0$, $\beta_x = 1.5$ (dotted curve), $\beta_e = 1.0$, $\beta_x = 3.0$ (continuous curve), and $\beta_e = \beta_x = 3.0$ (dot-dashed curve). Lower-panel: Radial evolution of the eigenvalue κ for the same cases shown in the upper panel.

compare the oscillated electron (anti)neutrino fluxes (at $r = 300 \text{ km}$) in the half-isotropic case ($\beta_e = \beta_x = 0$; dashed curve) with a non-trivial angular distribution with $\beta_e = 1.0$, $\beta_x = 1.5$ (thick dotted curve). The effect on the final spectra is dramatic: The spectral splits observable in the final ν_e spectra in the half-isotropic case are smeared-out and the spectral swaps are not complete.

In the upper panel of Fig. 2 we show the radial evolution of the z -component of the integrated value of the ν polarization vector P_z , that is related to the flavor content of the ensemble for four different angular distributions of Fig. 1. Namely, we compare the half-isotropic case ($\beta_e = 0$, $\beta_x = 0$, dashed curve) with three non-trivial angular distributions: $\beta_e = 1.0$, $\beta_x = 1.5$ (dotted curve), $\beta_e = 1.0$, $\beta_x = 3.0$ (continuous curve), and $\beta_e = \beta_x = 3.0$ (dot-dashed curve). First of all, note that with the $\beta_e = \beta_x = 3.0$ flavor-blind distributions the behavior does not present major changes with respect to the naive case, except from a delay in the start-

ing of flavor conversions at $r \simeq 90$ km. In the case of $\beta_e = 1.0$, $\beta_x = 1.5$, the onset of the flavor conversions (at $r \simeq 70$ km) is very close to what expected in the half-isotropic case ($r \simeq 75$ km). However, the further flavor evolution shows dramatic differences. Indeed, with the non-trivial angular distribution the final value of the integrated ν polarization vector would be $P_z \simeq 0$ indicating that the spectral differences between the final ν_e and ν_x spectra are strongly reduced with respect to the half-isotropic case. Choosing larger differences in the angular distributions of different flavors, as in the case with $\beta_e = 1.0$, $\beta_x = 3.0$, not only the final value of the P_z will change, but also flavor conversions would start much earlier ($r \simeq 55$ km) than in the half-isotropic case.

In the bottom panel of Fig. 2 we plot the radial evolution of the eigenvalue κ coming from the solution of Eq. (3) for the same cases shown in the upper panel. In the half-isotropic case $\beta_e = \beta_x = 0$ (dashed curve) the κ function presents a hump peaked around $r \simeq 100$ km and connected with a long tail around $r \simeq 75$ km. This tail indicates that the system is in principle always unstable. However, one can verify that in the tail the unstable ν frequency modes are in the infrared region, where the spectrum is strongly suppressed. Therefore, they have no impact for the flavor conversions. The onset of the flavor conversions is then given by the connection between the hump and the tail at $r = 75$ km. This result is in agreement with what shown in the numerical calculation of P_z , shown in the upper panel (dashed curve).

When considering non-trivial angular distributions, the long tail in the κ function in the half-isotropic case now disappears. However, the presence of a non-isotropic angular distribution is not enough to produce an enhancement in the value of κ . Conversely, in the flavor blind case $\beta_e = \beta_x = 3.0$ (dot-dashed curve) the instability is suppressed with respect to what has been seen in the half-isotropic case. In this case, flavor conversions start at $r = 80$ km. A significant enhancement of the multi-angle instability occurs when ν angular spectra exhibit crossing points in u , as can be seen in the case with $\beta_e = 1.0$, $\beta_x = 1.5$ (dotted curve) and even more in the one with $\beta_e = 1.0$, $\beta_x = 3.0$ (continuous curve). In both cases the peak in κ increases with respect to the half-isotropic case and also the hump broad-

ens toward smaller r . Since κ reaches a higher peak value, the width of the Lorentzian around an unstable frequency mode for a given angle u would be broad, implying a speed-up in the transitions. In particular, in the case of $\beta_e = 1.0$, $\beta_x = 1.5$ flavor conversions start at $r \simeq 70$ km, while in the case with $\beta_e = 1.0$, $\beta_x = 3.0$ around $r \simeq 55$ km, in agreement with the numerical results shown in the upper panel of Fig. 2.

Conclusions— We have described a new instability in self-induced flavor conversions for SN ν 's, associated with flavor-dependent angular distributions. These can lead to crossing points among the different spectra that can produce new flavor conversion effects, absent with an half-isotropic ν emission. We checked that this effect would develop in both the mass hierarchies and would be particularly relevant during the SN cooling phase, where the differences among the different flavors are relatively small, and self-induced effect can develop without any matter hindrance. The effect on the oscillated ν spectra can be dramatic. Namely, it would produce a smearing of the splitting features widely discussed in the half-isotropic case, and resulting ν fluxes with less significant spectral differences. This tendency toward spectral equalization would challenge the detection of further oscillation signatures, like the ones associated with the Earth crossing of SN ν 's (see, e.g., [19]). Moreover, we found that also onset of the flavor conversions can be significantly pushed at low-radii, challenging the multi-angle suppression found in the half-isotropic case [20]. Possible flavor conversions at low-radii would have an interesting impact on the r-process nucleosynthesis in SNe [21]. Furthermore, if ν oscillations develop too close to the neutrinosphere, they would invalidate the ν transport paradigm in SNe that ignores ν conversions. Given the importance of the effects discussed here, a future task would be to perform the flavor evolution and stability analysis taking into account angular distributions as realistic as possible, obtained directly from SN simulations.

Acknowledgements

We thank G. Raffelt for useful comments. The work of A.M. was supported by the German Science Foundation (DFG) within the Collaborative Research Center 676 ‘‘Particles, Strings and the Early Universe’’.

-
- [1] H. Duan *et al.*, Phys. Rev. D **74**, 105014 (2006).
 - [2] S. Hannestad *et al.*, Phys. Rev. D **74**, 105010 (2006) [Erratum-ibid. D **76**, 029901 (2007)].
 - [3] J. Pantaleone, Phys. Lett. B **287**, 128 (1992).
 - [4] Y. Z. Qian and G. Fuller, Phys. Rev. D **51**, 1479 (1995).
 - [5] H. Duan *et al.*, Ann. Rev. Nucl. Part. Sci. **60**, 569 (2010).
 - [6] H. Duan *et al.*, Phys. Rev. Lett. **99**, 241802 (2007).
 - [7] G. L. Fogli *et al.*, JCAP **0712**, 010 (2007).
 - [8] C. D. Ott *et al.*, Astrophys. J. **685**, 1069 (2008).
 - [9] S. Sarikas *et al.*, Phys. Rev. Lett. **108**, 061101 (2012).
 - [10] R. F. Sawyer, Phys. Rev. D **72**, 045003 (2005).
 - [11] B. Dasgupta *et al.*, Phys. Rev. Lett. **103**, 051105 (2009).
 - [12] A. Banerjee *et al.*, Phys. Rev. D **84**, 053013 (2011).
 - [13] A. Esteban-Pretel *et al.*, Phys. Rev. D **76**, 125018 (2007).
 - [14] G. G. Raffelt *et al.*, astro-ph/0303226.
 - [15] <http://prl.aps.org/supplemental/PRL/XXX>;
 - [16] A. Mirizzi, R. Tomas, Phys. Rev. **D84**, 033013 (2011).
 - [17] T.K. Kuo and J.T. Pantaleone, Rev. Mod. Phys. **61**, 937 (1989).
 - [18] S. Chakraborty *et al.*, Phys. Rev. Lett. **107**, 151101 (2011); Phys. Rev. D **84**, 025002 (2011).
 - [19] C. Lunardini and A. Y. Smirnov, Nucl. Phys. B **616**, 307

- (2001).
- [20] H. Duan and A. Friedland, Phys. Rev. Lett. **106**, 091101 (2011).
- [21] H. Duan *et al.*, J. Phys. G **G38**, 035201 (2011).